Journal of Applied Polymer Science

Silane-Modified NaA Zeolite/PAAS Hybrid Pervaporation Membranes for the Dehydration of Ethanol

Ping Wei,[1] Xinying Qu,[1] Hang Dong,[1] Lin Zhang,[1] Huanlin Chen,[1] Congjie Gao[1,2]

[1]Department of Chemical and Biological Engineering, Engineering Research Center of Membrane and Water Treatment Technology of MOE, Zhejiang University, Hangzhou 310027, People's Republic of China

[2]The Development Center of Water Treatment Technology, Hangzhou 310012, People's Republic of China

Correspondence to: L. Zhang (E-mail: linzhang@zju.edu.cn)

ABSTRACT: To improve the pervaporation selectivity of poly(acrylic acid) sodium (PAAS) membranes incorporated with NaA zeolite, the interface compatibility between zeolite nanocrystals and the polymer matrix was improved by modifying NaA zeolite using 3-aminopropyltriethoxysilane (APTES). Both X-ray photoelectron spectra and FTIR confirmed the chemical modification, while the results of zeolite particle size analysis and scanning electron microscopy revealed the improved dispersion of the modified zeolite. Transmission electron microscopy images of these hybrid membranes indicated that the interface between the polymer and modified zeolite phases had improved. The effects of loaded NaA zeolite on the pervaporation performance of hybrid membranes were investigated. The selectivity of hybrid membranes made from APTES-modified zeolite was higher than that using the original zeolite under the same conditions, because fewer voids resulted from the incompatibility between the zeolite and PAAS and the structure was more homogenous. Based on the Arrhenius plots, the activation energies of water and the ethanol ratio were lower for modified zeolite hybrid membranes, because water molecules experienced less restrictive passage through the membranes compared with the original zeolite-based hybrid membrane. © 2012 Wiley Periodicals, Inc. J. Appl. Polym. Sci. 000: 000–000, 2012

KEYWORDS: NaA zeolite; 3-amino-propyltriethoxysilane; poly(acrylic acid) sodium membrane; pervaporation dehydration

Received 1 May 2012; accepted 4 September 2012; published online

DOI: 10.1002/app.38555

INTRODUCTION

In recent years, organic–inorganic hybrid pervaporation membranes have received considerable attention because they combine the process ability of the organic polymer phase with the superior transport properties of the inorganic phase.[1–5] Common inorganic particles used in organic–inorganic hybrid membranes are usually silica,[6,7] zeolite,[8–10] carbon nanotubes,[11,12] and so on. Zeolite is often used as the inorganic filler in dehydration pervaporation membranes due to its excellent size-selective and polar nature.

However, many studies have found that there is an obstacle to the successful introduction of inorganic molecular sieve materials into an organic polymer matrix at the microscale because of the poor compatibility between zeolite and the polymer matrix.[13–15] Therefore, some methods have been proposed to improve the interfacial strength to enhance the separation performance. Surface modification of zeolite with silane coupling agents has been shown to be an effective method to increase the compatibility between the organic and inorganic phases of many composite materials, because free —Si—OH groups on the surface of zeolite possess high activity and may provide sites for the physical and chemical adsorption of silane coupling agents.[16,17] Duval et al.[18] demonstrated that the adhesion between the zeolite and glassy polymer matrix phases could be improved by modifying the zeolite surface with amino functional silane-coupling agents. However, there was no significant improvement in permselectivity, although scanning electron microscopy (SEM) micrographs indicated good coupling between silane and zeolite. This may have occurred due to the lack of a reaction between the amino group of the coupling agent and the polymer chain. Sun et al.[19] used 3-mercapto-propyl-trimethoxysilane (MPTMS) as a silylation agent to modify the surface of H-ZSM-5 zeolite. The experimental results indicated good coupling between silane and zeolite; meanwhile, the modification eliminated the nonselective voids at the interface of chitosan and H-ZSM-5 via ion–ion interactions. As such, the modified H-ZSM-5-filled membranes showed much higher selectivity. However, the preparation method was complicated. —SH groups introduced by MPTMS on the surface of H-ZSM-5 need to be further oxidized at 25°C in 30 wt % H_2O_2 for 24 h to convert into —SO_3H groups that can react with amido groups on the adjacent chitosan chains.

Applied Polymer SCIENCE

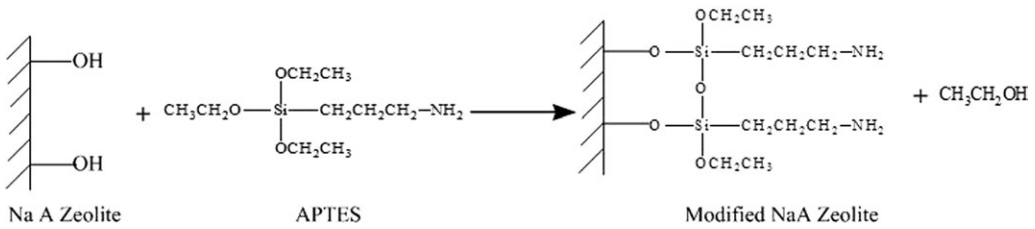

Figure 1. Schematic diagram of the reaction mechanism.

The objective of this work was to attempt to modify NaA zeolite using amino-terminated silane-coupling 3-aminopropyltriethoxysilane (APTES). The amino group on the surface of modified zeolite introduced by APTES can directly react with carboxyl groups in poly(acrylic acid) sodium (PAAS) via acid–base ion–ion interactions, thus increasing the compatibility between zeolite and the polymer. By comparing the morphology and separation performance of membranes loaded with either the original or the modified zeolite, the role of compatibility in hybrid membrane performance and the related mechanisms were investigated.

EXPERIMENTAL

Materials and Chemicals

PAAS (MW: 300,0000) and ethanol were purchased from Sinopharm Chemical Reagent, China. APTES was bought from Tokyo Kasei, Japan. Polyacrylonitrile ultrafiltration (PAN) membranes (MWCO: 20,000) were used as the support and were supplied by the Department Center of Water Treatment Technology, Hangzhou, China. A-type zeolite (NaA) was synthesized in the laboratory. Sodium aluminate ($NaAlO_2$, 99.9%) was purchased from Strem Chemicals. Tetrapropylammonium hydroxide ($NaSiO_3.9H_2O$, 99 wt %) was purchased from Aldrich. Deionized water was used in all experiments.

Synthesis of NaA Zeolite

The NaA particles were synthesized by mixing a solution with a molar composition of $Na_2O : SiO_2: Al_2O_3 : H_2O = 4.9 : 1.6 : 1 : 173$ in a sealed polypropylene bottle. This mixture was stirred for 24 h and then heated at 40°C under vapor reflux for 10 days. After the reaction mixture had cooled, zeolite was separated from the solution by repeated cycles of 1 h of centrifugation at 12,000 rpm. The resulting concentrated product solution was dried on a hot plate at 60°C and then calcined in air at 550°C for 12 h (1°C min^{-1}).

Surface Modification of NaA Zeolite

Surface modification processes have been reported previously.[20] First, a mixture of toluene (100 mL), APTES (6 mL), and NaA zeolite (1 g) was stirred in an enclosed N_2 environment at 110°C for 6 h. Then, the product was filtered with 250 mL of toluene and washed with 250 mL of ethanol to remove the unreacted silane. Finally, the modified zeolite was dried under vacuum at 110°C for 1 h. A schematic of the reaction is shown in Figure 1.

Membrane Preparation

PAAS/zeolite hybrid membranes were fabricated by the solution casting method. Specific amounts of zeolite were distributed in deionized water and redispersed under ultrasonication for 20 min. Afterward, the PAAS was added to the zeolite solution. The weight fraction of zeolite in the PAAS matrix was varied from 0 to 15 wt % and the solute concentration of the casting solutions was adjusted to 1.5 wt %. After stirring at room temperature for 72 h, homogeneous casting solutions were obtained. The solution was cast onto the PAN UF membrane, which was previously fixed on glass plates, with the aid of a casting knife. The cast membranes were heated at 50°C for 2–3 h and then at room temperature for 12 h, and PAAS/zeolite hybrid membranes were obtained.

Characterization

The FTIR spectra of the original and modified NaA zeolite particles were obtained on a Tenson27 spectrophotometer (Bruker Germany) by the diffused reflectance (DRIFT) method. The size distribution of NaA zeolites was measured by a particle size analyzer (Otsuka Electronic, LPA-3000) using the dynamic light scattering method. X-Ray photoelectron spectra (XPS) of the original and modified NaA zeolite particles were measured using a Kratos Axis Ultra DLD instrument (Shimadzu-KRATOS, Japan) equipped with a CuKα ($\lambda = 0.154$ nm) radiation source. Surface morphologies of the membranes were examined by SEM (SIRION-100, FEI, Hillsboro, OR) at an accelerated voltage of 25 kV and by transmission electron microscopy (TEM) (JEM-1200EX, JEOL, Japan) to determine if the zeolite particles were dispersed homogenously and if voids existed between the polymer and zeolite phases.

PV Measurements

In the experiment, a flat-sheet membrane with an effective area of 18.1 cm^2 was installed at the center of the membrane module for the evaluation of water/ethanol separation performance. This process has been reported in the literature.[20] An aqueous solution of ethanol was continuously circulated from the feed tank to the upstream side of the membrane. The temperature of the feed mixture was kept constant by means of a water jacket with a thermostat at 30°C. The vacuum on the downstream side was maintained at about 135 Pa by a vacuum pump. The permeate was collected in a cold trap. The compositions of the permeate and the feed were determined on a gas chromatograph (GC-950, China) equipped with a 2.0-m-long column packed with Porapak Q and a TCD detector with the column temperature set to 120°C. From the collected amount and composition of the permeate, the permeation flux and separation factor can be obtained. The permeation flux and separation factor were calculated by the following equations:

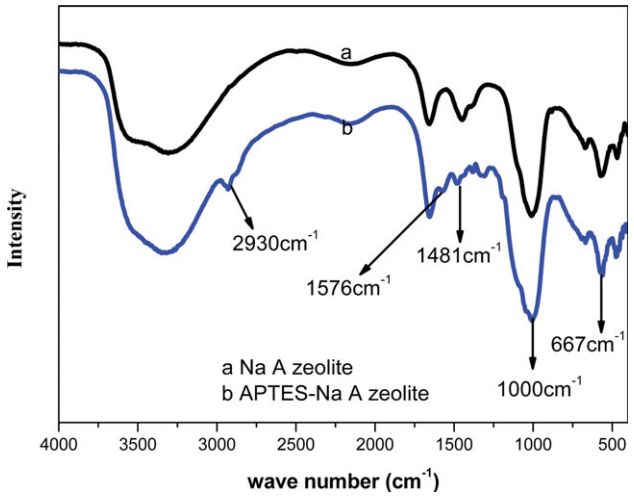

Figure 2. FTIR spectra of (a) NaA zeolite and (b) APTES-modified NaA zeolite. [Color figure can be viewed in the online issue, which is available at wileyonlinelibrary.com.]

$$J = \frac{\Delta g}{S \times \Delta t} \quad (1)$$

$$\alpha = \frac{P_{\text{ethanol}}/P_{water}}{F_{\text{ethanol}}/F_{water}} \quad (2)$$

where Δg is the permeation weight collected in the cold trap during the operation time Δt and S is the membrane area (18.1 cm^2). F_{ethanol} and F_{water} are the weight fractions of ethanol and water in the feed (wt %), and P_{ethanol} and P_{water} are the weight fractions in the permeate (wt %), respectively.

RESULTS AND DISCUSSION

FTIR Spectra of Zeolite

FTIR spectra of zeolite and modified zeolite are shown in Figure 2. The bands at 1000 and 667 cm^{-1} corresponded to the Si—O asymmetric and symmetric stretching vibrations in the spectrum of NaA zeolites. The peak at 3467 cm^{-1} corresponded to the inner-hydroxyl group. The characteristic peaks (2930, 1576, and 1481 cm^{-1}) of the grafted groups were present in the FTIR spectra of the modified zeolite in Figure 1(b). These typical bands (stretching, 2930 cm^{-1} and bending, 1481 cm^{-1}) belonged to aliphatic C—H, whereas the vibrations of the amine species (N—H) were visible at 1576 cm^{-1}. Thus, the IR data demonstrate that the surface of the NaA zeolites was successfully modified without altering the zeolite structure.

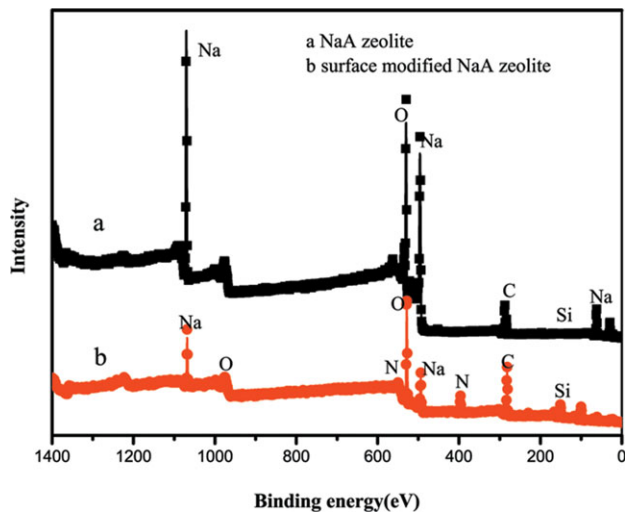

Figure 3. XPS of NaA zeolite before (a) and after (b) surface modification. [Color figure can be viewed in the online issue, which is available at wileyonlinelibrary.com.]

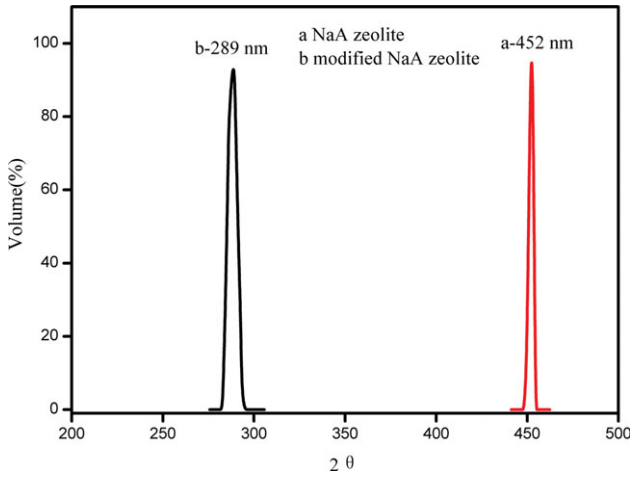

Figure 4. Diameter distribution of NaA zeolite in water before and after surface modification. [Color figure can be viewed in the online issue, which is available at wileyonlinelibrary.com.]

XPS Analysis of Zeolite

The XPS spectra of the original and modified zeolite are shown in Figure 3. After modification, a new peak clearly appeared at 398.2 eV that was attributed to the nitrogen atom of the silane coupling agent containing an amino group. Another new peak at 284.3 eV also appeared in Figure 3(b), which was attributed to the —CH group of APTES. The results in Figure 3 indicate that some molecules of the silane coupling agent had been grafted onto the external surface of the zeolite.

Zeolite Particle Size Analysis

The particle size distributions of the original and modified NaA zeolites shown in Figure 4 were used to indicate their relative dispersion. When deionized water was used as the dispersion medium, the mean particle sizes of NaA zeolites before and after modification were 452 and 289 nm, respectively. The original zeolites in neutral water aggregated due to the lack of a force to prevent the particles from coming together. However, primary amine groups were introduced to the particles by silanization with APTES. The solution showed alkalescence and the amino groups on the surface of the modified zeolites became positively charged. The solution also showed ionization of $—NH_2$, namely, the formation of NH_3^+ on the surface of the zeolite particles. Therefore, the modified NaA zeolites repelled each other, resulting in dispersion stability, which agrees with the results obtained by Schiestel.[21] As a result, the dispersion of the zeolites in water was significantly improved after the surface was modified.

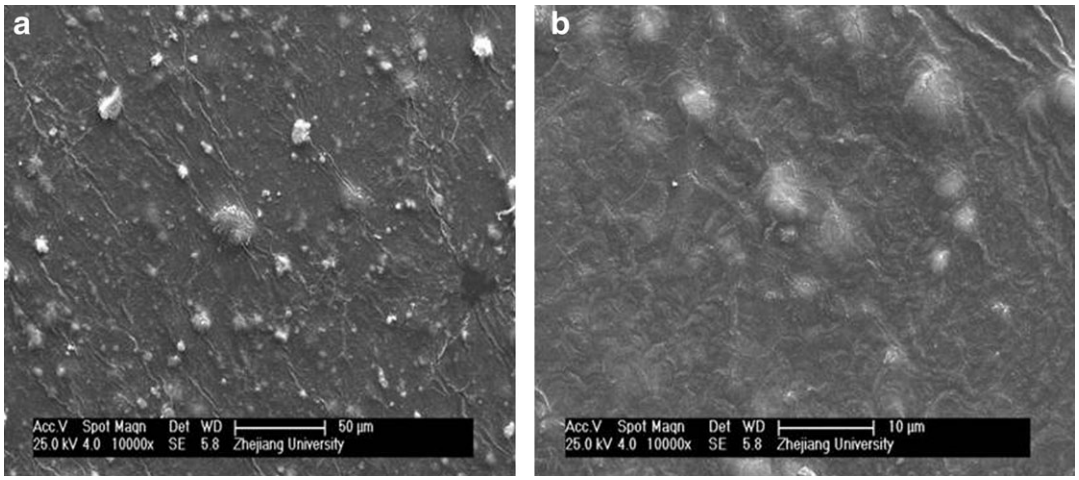

Figure 5. Comparison of SEM images of PAAS/zeolite hybrid membranes loaded with 10 wt % NaA zeolites before (a) and after (b) surface modification.

Membrane Formation and Morphology

The surface morphologies of the hybrid membranes loaded with original and modified zeolites are shown in Figures 5 and 6, respectively. Before the zeolite was modified, the poor adhesion between polymer and zeolite was likely the cause of zeolite aggregation in the hybrid membrane, as shown in Figures 5(a) and 6(a). Moreover, some macrovoids formed at the interface between the original zeolite and the polymer matrix in the hybrid membrane. In contrast, the membranes loaded with modified zeolites were observed to be more homogeneous, as shown in Figures 5(b) and 6(b), and there were no voids in the hybrid membrane. After the zeolite surface was modified, the $-NH_3^+$ groups on the surface-modified NaA introduced by the silane coupling agent interacted with $-COO^-$ groups on PAAS via electrostatic forces. Ion–ion interaction improves the compatibility between different materials.[22,23] Therefore, it can be deduced that ion–ion interactions play an important role in improving the compatibility between the polymer matrix and the inorganic phase. In addition, the dispersion of the modified zeolite was improved, so the membranes became more homogenous.

Effect of Zeolite Loading on Pervaporation Performance

Figure 7 shows the investigation of the separation behavior of the hybrid membranes using a 90 wt % aqueous ethanol solution filled, membranes were loaded with either the original or the modified NaA zeolite. With increased zeolite loading, the permeation flux decreased and the separation factor increased. These results can be explained by the reduced permeability region within the sieve surface with zeolite loading[24] and the reduced valid transport space of the polymer through which molecules may diffuse. Similar results have been reported by Kittur et al. and Yeh et al.[25,26] They explained that the addition of the inorganic material reduces the free volume through which molecules may diffuse. On the other hand, the loaded NaA zeolite enhanced the hydrophilicity and molecular sieving

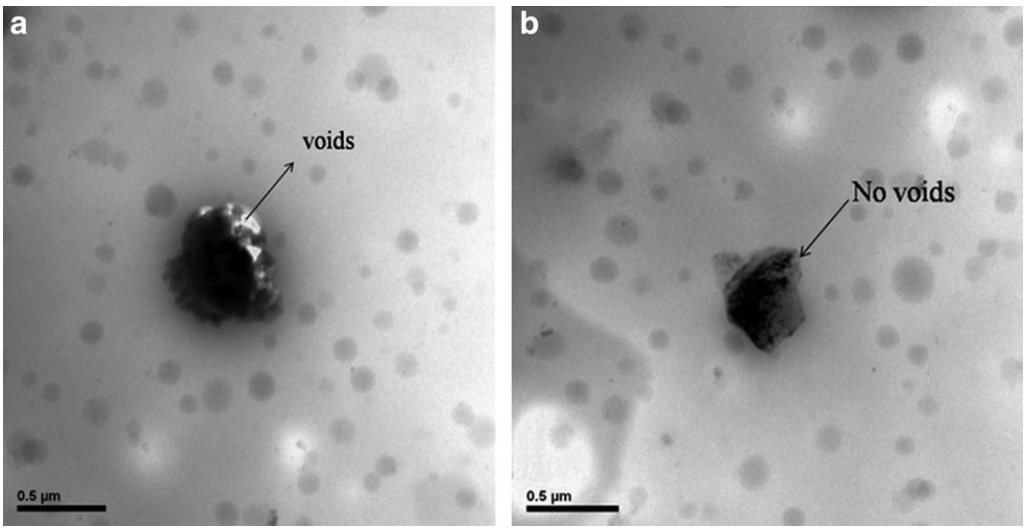

Figure 6. Comparison of TEM images of PAAS/zeolite hybrid membranes loaded with 10 wt % NaA zeolites before (a) and after (b) surface modification.

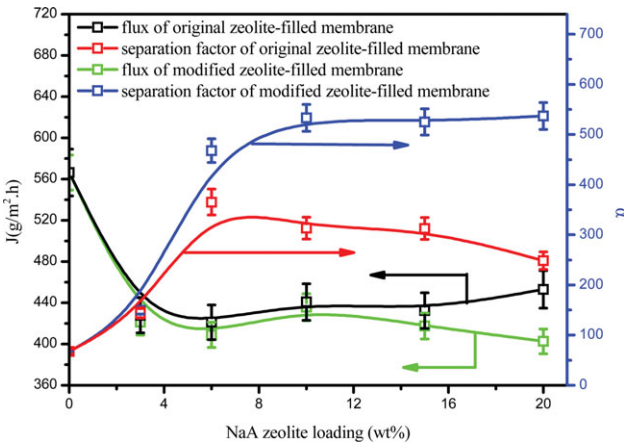

Figure 7. Effect of zeolite loading on pervaporation performance of PAAS/NaA hybrid membranes for the dehydration of a 90 wt % aqueous ethanol solution at an operation temperature of 30°C. [Color figure can be viewed in the online issue, which is available at wileyonlinelibrary.com.]

action of the hybrid membrane; thus, water can penetrate along the straight path while ethanol cannot pass through the pores.

However, for the hybrid membrane loaded with the original zeolite, the separation factor clearly decreased when zeolite loading exceeded 6 wt % due to the formation of more interfacial voids resulting from the aggregation of zeolite. Ethanol can pass through these voids and, as a result, more ethanol permeates through the membrane. Meanwhile, the molecular sieving action of zeolite was decreased as a result of aggregation. In comparison, when modified zeolite loading exceeded 6 wt %, the separation performance was still excellent because of better compatibility and dispersion. An illustration of the proposed transport path with different amounts of zeolite in the membrane is shown in Figure 8.[27]

In this experiment, the best performance obtained was a separation factor of 533.2 with the 10 wt % modified zeolite-loaded hybrid membrane. These performance results were better than for the original zeolite-loaded hybrid membrane. The results of this work were compared with other hybrid membranes reported in the literature, as shown in Table I and Figure 9. It can be seen that the separation factor of the modified NaA/PAAS was higher, and the shaded area was considered the better performance for application. The performance data obtained in this work are close to the shaded area. Moreover, our modified approach is simple and feasible. The modified NaA zeolites can directly interact with the PAAS, and the polymer does not require further chemical modification.

Effect of Operation Temperature on Pervaporation Performance

In pervaporation, one of the important parameters affecting the separation performance of the membrane is operation temperature. The effect of operation temperature on PV performance was studied with an aqueous ethanol solution of 10 wt % water; the results are presented in Figure 10. With the operation temperature increasing from 30 to 100°C, for both the modified and original zeolite-filled membranes, it can be observed that the permeation flux increased and the separation factor decreased. Nevertheless, the separation factor was obviously higher for the modified zeolite-filled membranes. Traditionally, this is explained by thermal agitation, because the polymer segments are more mobile and thus facilitate transport of the permeants through the membrane. Meanwhile, as the feed temperature increases, vapor pressure in the feed compartment increases, but vapor pressure on the permeate side is not affected. This would result in an increased driving force with increasing temperature. The driving force is closely related to the phase transition in the PV process and thus, is strongly dependent on the operating temperature. This affects the membrane performance in such a

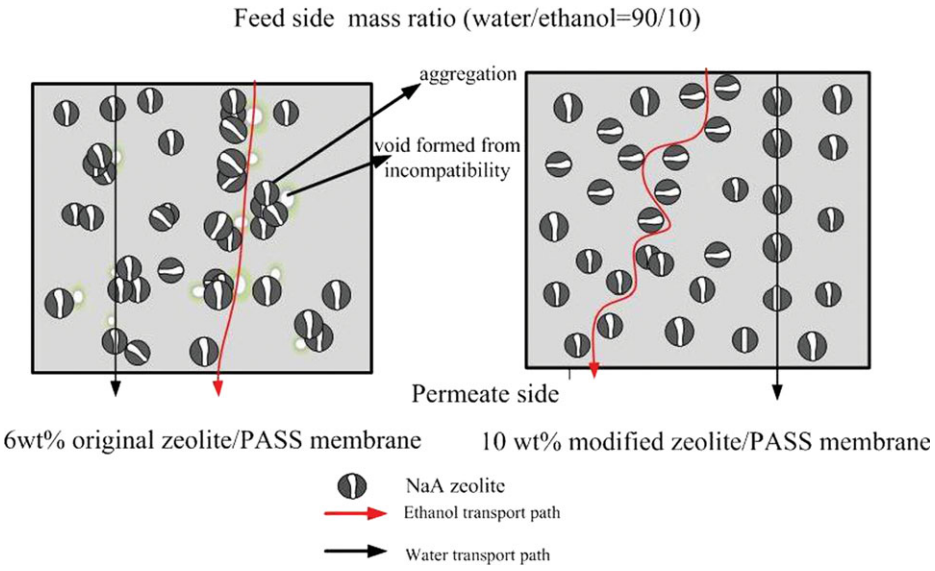

Figure 8. Illustration of the proposed transport path for NaA zeolite membranes. [Color figure can be viewed in the online issue, which is available at wileyonlinelibrary.com.]

Table I. Dehydration of Ethanol Using Mixed Matrix Membranes (Results from the Literature and the Present Study)

Water concentration (wt %)	Separation layer	Separation factor	Flux (g m^{-2} h^{-1})	Temperature (°C)	References
10	H-ZSM-5/M(24)-CS	54.18	158.02	80	9
5	PVA/clay	58	57	Not given	25
5	PVA/clay	112	39	Not given	25
30	PDMS/silicalite-1	43.6	513	22	28
30	PDMS/silicalite-1	13.6	527	22	28
35	PDMS/silicalite-1	16	145	22	28
49	PDMS/silicalite-1	33.5	150	22	28
20	PVA	15.5	183	50	29
20	PVA/11 wt % KA zeolite	15.5	235	50	29
20	PVA/11 wt % NaA zeolite	13.8	258	50	29
20	PVA/11 wt % CaA zeolite	10.4	323	50	29
20	PVA/11 wt % NaX zeolite	8.5	376	50	29
8	PAN	281	7	50	30
8.7	PAN/25 wt % zeolite X	35.9	54	50	30
9	PAN/32 wt % zeolite X	51.9	88	50	30
7	PAN/40 wt % zeolite X	3.2	369	50	30
8.5	PAN/50 wt % zeolite X	7.1	277	50	30
10	Polyamide	26	380	25	31
10	Polyamide/SDS clay	12	280	25	31
10	CS/H_{14}-P_5 nanoparticle	35 991	113	30	32
10	PSf/44 wt % 4 A zeolite	351	175	25	33
10	NaAlg/10 wt % Beta	1,598	132	30	34
12	NR/PAA/10 wt % 4 A zeolite	41,600	1977	30	35
10	PAAS/original NaA zeolite	313.2	440.8	30	This work
10	PAAS/modified NaA zeolite	435.7	533.2	30	This work

way that the flux was increased, but selectivity is decreased with an increase in temperature.[36,37]

For hybrid membranes, the unselective void region between the polymer and the zeolite are involved in a complex interplay of physical and chemical factors, such as the expansion coefficient.[38] As the operation temperature increases, the expansion coefficient of the PAAS matrix and the zeolite become different, so the

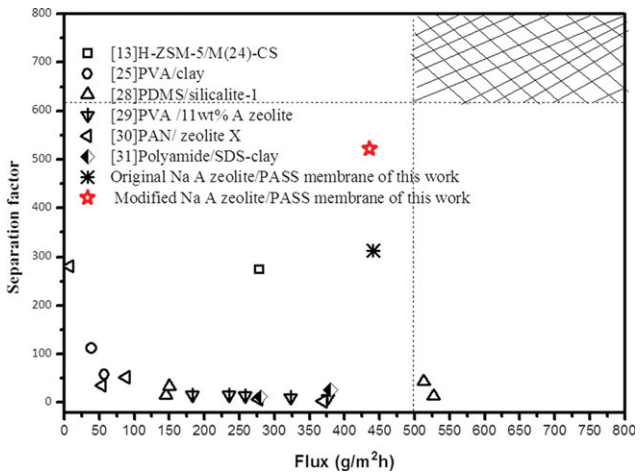

Figure 9. Performance comparison of the dehydration of ethanol using hybrid membranes. [Color figure can be viewed in the online issue, which is available at wileyonlinelibrary.com.]

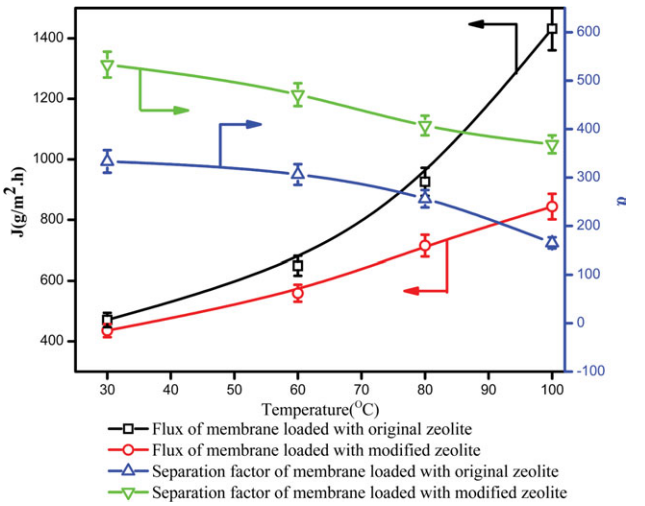

Figure 10. Effect of an operating temperature on pervaporation performance at 90 wt % ethanol in the feed for 10 wt % NaA zeolite-loaded hybrid membranes. [Color figure can be viewed in the online issue, which is available at wileyonlinelibrary.com.]

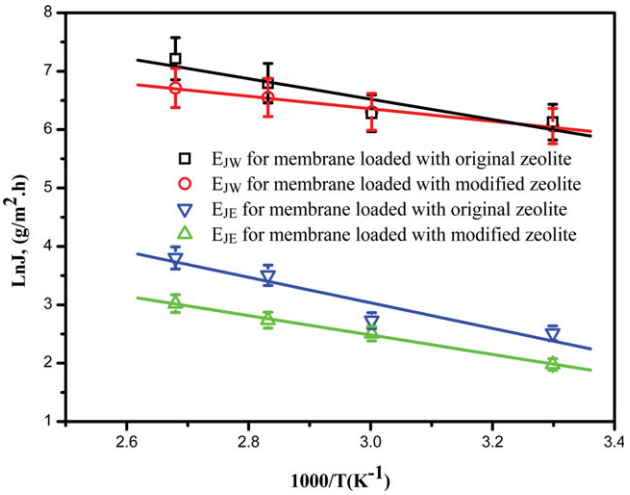

Figure 11. Arrhenius plots of hybrid PAAS membranes. [Color figure can be viewed in the online issue, which is available at wileyonlinelibrary.com.]

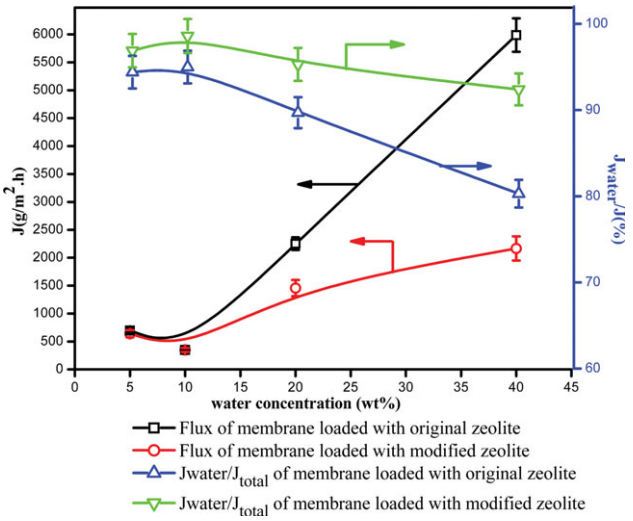

Figure 12. Effect of water concentration on the pervaporation performance for 10 wt % modified NaA/PAAS hybrid membranes at an operation temperature of 30°C. [Color figure can be viewed in the online issue, which is available at wileyonlinelibrary.com.]

nonselective voids become larger and the ethanol permeates through the membrane more easily. Based on these three reasons, the permeation flux increased, but the separation factor decreased.

The relationship between permeation flux and operation temperature was analyzed by the Arrhenius equation as follows:

$$J = A_J \exp\left(-\frac{E_J}{RT}\right) \quad (3)$$

where A_J is the frequency factor and E_J is the permeation activation energy.

Arrhenius plots are presented in Figure 11, and the permeation activation energy for water and ethanol were obtained as shown in Table II. With these data, it was observed that the activation energy values of both water and ethanol were higher before surface modification because of the aggregation of zeolites. The apparent activation energy values of water (E_{JW}) were lower than those of ethanol (E_{JE}), suggesting that the hybrid membranes had significantly higher separation efficiency. Obviously, after the zeolite surface was modified, the E_{JW}/E_{JE} became lower, so the separation factor of the modified hybrid membranes was higher than the original hybrid membranes.

Effect of Water Concentration on Pervaporation Performance

The effect of water concentration on the pervaporation performance of 10 wt % original and modified NaA-filled membranes at 30°C was investigated; the results are shown in Figure 12. In general, flux clearly increased for the hybrid membranes loaded with the original and modified zeolit when a concentration of preferential permeating specie in feed is high, it is commonly explained that membranes experience an extensive swelling that leads to expanded polymeric networks with a consequence of increased permeation of less-permeating component the permeation.[39–41] When the water composition in the feed was 40 wt %, the water permeate composition was about 80 wt % for the membrane loaded with the original zeolite, while the water composition for the membrane with modified zeolite was above 92% and the permeation flux also increased to more than 2000 g m^{-2}·h^{-1}.

It was found that the total permeation flux increased almost exponentially for the hybrid membrane with an increasing composition of water in the feed. If enough water is present inside the membrane, the zeolite pores will be largely occupied by water molecules, prohibiting ethanol molecules from entering the pores of the zeolite;[42–47] hence, the permeation flux of hybrid membranes is high and the water concentration in the permeate is slightly lower. However, a very destructive force affecting adhesion appeared with the migration of water to the hydrophilic surface of the inorganic reinforcement. Water interrupts the interface, destroying the bonds between the polymer and the adhesion between the polymer and the zeolite. Thus, ethanol could permeate through macrovoids in the membrane. However, for the modified zeolite-filled membrane, the J_{water}/J_{total} of the hybrid membrane increased due to the amino silane introduced by the silane coupling agent. The amino silane could create a water-resistant bond at the interface between the zeolite NaA and PAAS.

Table II. Arrhenius Activation Parameters for Permeation (KJ mol^{-1})

Arrhenius activation parameters for permeation (kJ mol^{-1}) according to membrane type	E_{JW} (water) (kJ mol^{-1})	E_{JE} (ethanol) (kJ mol^{-1})
$M_{original}$	15.85	18.19
$M_{modified}$	8.90	14.82

CONCLUSIONS

The NaA zeolite was successfully modified by ATPES and incorporated into PAAS membranes for the pervaporation dehydration of ethanol. As result of surface modification of the zeolite, the dispersion of zeolite in the hybrid membrane was improved and the morphology of the hybrid membrane was more homogeneous. The separation performance of the hybrid membrane was also enhanced. An obvious

increase in separation, with 533.2 for the modified NaA/PASS membrane compared to 313.2 for the original NaA/PASS membrane, was observed under identical conditions. The operation temperature and water composition in the feed played a significant role in permeate flux and the separation factor. The permeation flux increased sharply and the separation factor decreased for the hybrid membranes, but the separation factor could be improved when the loaded zeolite surface was surface modified.

ACKNOWLEDGMENTS

This project is sponsored by the National High Technology Research and Development Program of China (2009AA02Z208), the National Basic Research Program of China (2009CB623402), and the Fundamental Research Funds for the Central Universities.

REFERENCES

1. Guizard, C.; Bac, A.; Barboiu, M.; Hovnanian, N. *Sep. Purif. Technol.* **2001,** *25*, 167.
2. Merkel, T. C.; Freeman, B. D.; Spontak, R. J.; He, Z.; Pinnau, I.; Meakin, P.; Hill, A. *J. Sci.* **2002,** *296*, 519.
3. Uragami, T.; Okazaki, K.; Matsugi, H.; Miyata, T. *Macromolecules* **2002,** *35*, 9156.
4. Liu, J. S.; Ma, Y.; Hu, K. Y.; He, H. M.; Shao, G. Q. *J. Appl. Polym. Sci.* **2010,** *117*, 2464.
5. Shirazi, Y.; Ghadimi, A.; Mohammadi, T. *J. Appl. Polym. Sci.* **2012,** *124*, 2871.
6. Liu, Y. L.; Hsu, C. Y.; Su, Y. H.; Lai, J. Y. *Biomacromolecules* **2005,** *6*, 368.
7. Claesa, S.; Vandezande, P.; Mullensa, S.; De Sitter, K.; Peeters, R.; Van Bael, K. M. *J. Membr. Sci.* **2012,** *389*, 265.
8. Huang, Z.; Guan, H. M.; Tan, W. L.; Qiao, X. Y.; Kulprathipanja, S. *J. Membr. Sci.* **2006,** *276*, 260.
9. Mosleh, S.; Khosravi, T.; Bakhtiari, O.; Mohammadi, T. *Chem. Eng. Res. Des.* **2012,** *90*, 433.
10. Prasad, C. V.; Yeriswamy, B.; Sudhakar, H.; Sudhakara, P.; Subha, M. C. S.; Song, J. I.; Rao, K. C. *J. Appl. Polym. Sci.* **2012,** *125*, 3351.
11. Liu, Y. L.; Chen, W. H.; Chang, Y. H. *Carbohydr. Polym.* **2009,** *232*, 23.
12. Qiu, S.; Wu, L. G.; Shi, G. Z.; Zhang, L.; Chen, H. L.; Gao, C. *J. Ind. Eng. Chem. Res.* **2010,** *49*, 11667.
13. Sun, H. L.; Lu, L. Y.; Peng, F. B.; Wu, H.; Jiang, Z. Y. *Sep. Purif. Technol.* **2006,** *52*, 203.
14. Moore, T. T.; Mahajan, R.; Vu, D. Q.; Koros, W. *J. AIChE J.* **2004,** *50*, 311.
15. Mahajan, R.; Burns, R.; Schaeffer, M.; Koros, W. J. *J. Appl. Polym. Sci.* **2002,** *86*, 881.
16. Zhou, H. L.; Su, Y.; Chen, X. R.; Yi, S. L.; Wan, Y. H. *Sep. Purif. Technol.* **2010,** *75*, 286.
17. Li, Y.; Guan, H. M.; Chung, T. S.; Kulprathipanja, S. *J. Membr. Sci.* **2006,** *275*, 17.
18. J. M.; Kemperman, A. J. B.; Folkers, B.; Mulder, M. H. V.; Desgrandchamps, G.; Smolders, C. A. *J. Appl. Polym. Sci.* **1994,** *54*, 409.
19. Sun, H. L.; Lu, L. Y.; Chen, X.; Jiang, Z. Y. *Appl. Surf. Sci.* **2008,** *254*, 5367.
20. Qu, X. Y.; Dong, H.; Zhou, Z. J.; Zhang, L.; Chen, H. L. *Ind. Eng. Chem. Res.* **2010,** *49*, 7504.
21. Schiestel, T.; Brunner, H.; Tovar, G. E. M. *J. Nanosci. Nanotechnol.* **2004,** *4*, 504.
22. Slisenko, O.; Lebedev, E.; Pissis, P.; Spanoudake, A.; Kontou, E.; Grigoryeva, Q. *J. Therm. Anal. Calorim.* **2006,** *84*, 15.
23. Al-Salah, H. *Polym. Bull.* **1998,** *40*, 477.
24. Moore, T. T.; Koros, W. J. *J. Mol. Struct.* **2005,** *739*, 87.
25. Yeh, J.-M.; Yu, M.-Y.; Liou, S.-J. *J. Appl. Polym. Sci.* **2003,** *89*, 3632.
26. Kittur, A. A.; Kariduraganavar, M. Y.; Toti, U. S.; Ramesh, K.; Aminabhavi, T. M. *J. Appl. Polym. Sci.* **2003,** *90*, 2441.
27. TeHenneppe, H. J. C.; Bargeman, D.; Mulder, M. H. V.; Smolders, C. A. *J. Membr. Sci.* **1987,** *35*, 39.
28. Jia, M. D.; Peinemann, K. V.; Behling, R. D. *J. Membr. Sci.* **1992,** *73*, 119.
29. Gao, Z.; Yue, Y.; Li, W. *Zeolites* **1996,** *16*, 70.
30. Okumus, E.; Urkan, T. G.; Yilmaz, L. *J. Membr. Sci.* **2003,** *223*, 23.
31. Wang, Y. C.; Fan, S. C.; Lee, K. R.; Li, C. L.; Huang, S. H.; Tsai, H. A.; Lai, J. Y. *J. Membr. Sci.* **2004,** *239*, 219.
32. Magalad, V. T.; Gokavi, G. S.; Nadagouda, M. N.; Aminabhavi, T. M. *J. Phys. Chem. C* **2011,** *115*, 14731.
33. Fu, Y. J.; Hu, C. C.; Lee, K. R.; Lai, J. Y. *Desalination* **2006,** *193*, 119.
34. Adoor, S. G.; Manjeshwar, L. S.; Bhat, S. D.; Aminabhavi, T. M. *J. Membr. Sci.* **2008,** *318*, 233.
35. Amnuaypanich, S.; Naowanon, T.; Wongthep, W.; Phinyocheep, P. *J. Appl. Polym. Sci.* **2012,** *124*, E319.
36. Fujita, H.; Kishimoto, A.; Matsumoto, K. M. *Trans. Faraday Soc. 1660*, 56, 424.
37. Adoor, S. G.; Prathab, B.; Manjeshwar, L. S.; Aminabhavi, T. M. *Polymer* **2007,** *48*, 5417.
38. Kariduraganavar, M. Y.; Kittur, A. A.; Kulkarni, S. S.; Ramesh, K. *J. Membr. Sci.* **2004,** *238*, 165.
39. Wang, L.; Li, J.; Lee, Y.; Chen, C. *Chem. Eng. J.* **2009,** *146*, 71.
40. Chen, X.; Yang, H.; Gu, Z.; Shao, Z. *J. Appl. Polym. Sci.* **2001,** *79*, 1144.
41. Guo, W. F.; Chung, T. S.; Matsuura, T. *J. Membr. Sci.* **2004,** *245*, 199.
42. Smit, B.; Maesen, T. L. M. *Chem. Rev.* **2008,** *108*, 4125.
43. Kittur, A. A.; Kulkarni, S. S.; Aralaguppi, M. I.; Kariduraganavar, M. Y. *J. Membr. Sci.* **2005,** *247*, 75.
44. Van den Berg, A. W. C.; Gora, L.; Jansen, J. C.; Makkee, M.; Maschmeyer, T. *J. Membr. Sci.* **2003,** *224*, 29.
45. Su, Y. H.; Liu, Y. L.; Sun, Y. M. *J. Membr. Sci.* **2007,** *296*, 21.
46. Kondo, M.; Komori, M.; Kita, H.; Okamoto, K. *J. Membr. Sci.* **1997,** *133*, 133.
47. Okamoto, K.; Kita, H.; Horii, K.; Tanaka, K. *Ind. Eng. Chem. Res.* **2001,** *40*, 163.